Journal of Statistical Physics, Vol. 69, Nos. 5/6, 1992

Monte Carlo Calculations of the Conformal Charge

Xidi Wang[1] **and George A. Baker, Jr.**[2]

Received December 5, 1991

The conformal charge is an important quantity which characterizes the nature of the two-dimensional phase transition. We report a first attempt to use a new numerical method to calculate the conformal charge. In this paper, we apply our method to the 2-dimensional, ϕ^4, continuous-spin Ising model. By varying the parameters in the Hamiltonian, one can change continuously from the known Gaussian limit to the Ising limit. It is well known that the critical points for these two systems are not in the same universality class. We study this behavior for the Gaussian model, the single-well ϕ^4 model, the border model, and the double-well ϕ^4 model for a large lattice. Our results, while giving a good general picture, are not so far sufficient to differentiate whether the non-Gaussian cases studied belong to the Ising model universality class or not. Further studies of other lattice sizes should serve to improve greatly our conclusions.

KEY WORDS: Monte Carlo simulations; conformal charge; central charge; conformal invariance; continuous-spin Ising model; critical phenomena; parallel computers.

1. INTRODUCTION AND SUMMARY

A major advance in the theory of two-dimensional (2D) critical phenomena has been the introduction of the conformal invariance hypothesis. So far as we know, no counterexamples have been discovered. This idea is an extension of the scaling hypothesis, and is also called "local scale invariance." The seminal papers in this area are those of Belavin *et al.*,[1] Cardy,[2] and Friedan *et al.*[3] In these works it was recognized that

[1] Center for Nonlinear Studies, Los Alamos National Laboratory, University of California, Los Alamos, New Mexico 87545.

[2] Theoretical Division, Los Alamos National Laboratory, University of California, Los Alamos, New Mexico 87545.

0022-4715/92/1200-1069$06.50/0

the only possible conformally invariant critical theories are broadly categorized by a parameter called the central charge. Furthermore, the only possible values of this charge are

$$c = 1 - \frac{6}{m(m+1)}, \qquad m = 2, 3, \ldots, \qquad \text{and} \quad c \geqslant 1 \tag{1}$$

Until recently the central charge c, which is characteristic of bulk critical phenomena, could only be inferred either from finite-size corrections[4–6] or indirectly through comparison with the table of possible cases.[3] Recently, following the discovery by Zamolodchikov[7] of his c-theorem and the work of Cardy,[8] the notion of conformal invariance has been extended beyond the critical point. Singh and Baker[9] have shown that these results can be used to compute the central charge of a conformally invariant theory directly from bulk properties as a particular hyperuniversal amplitude ratio. They demonstrated this possibility with a high-temperature series approach. We will often refer to the central charge c, which is of course the structure constant multiplying, in the relation between the infinitesmal generators, the algebraic center of the Virasoro algebra induced by conformal invariance, as the conformal charge, to emphasis both concepts in a shorthand way. It is the purpose of this paper to report on the application of Monte Carlo methods to this problem.

We shall treat as our problem of interest the 2D continuous-spin Ising model. In this model, the interaction energy is proportional to a sum over nearest neighbors (i, j) of the product of the spin variables $\phi_i \phi_j$, and the spin distribution is proportional to $\exp(-A\phi^2 - G\phi^4)$. By a variation of parameters, one can move continuously from the Gaussian model to the spin-1/2 Ising model. For the Gaussian model, the conformal charge can be shown[10] to be $c = 1$. The critical exponents are $\alpha = 1$ for the index of divergence of the specific heat, $\gamma = 1$ for the index of divergence of the magnetic susceptibility, $\nu = 1/2$ for the index of divergence of the correlation length, and $\eta = 0$ for the index of the two-point correlation function at the critical temperature. At the other extreme, the Ising model, we know that[3] $c = 1/2$, $\alpha = 0$ (logarithmic divergence), $\beta = 1/8$ for the index of convergence of the spontaneous magnetization, $\gamma = 1.75$, $\nu = 1$, and $\eta = 1/4$. The continuous-spin Ising model is of interest in its own right. Many workers had thought for some time that as long as $G > 0$, the critical properties of this model were in the Ising model universality class. However, Baker and Johnson[11] pointed out that there are reasons to believe that the border model (the case where $A = 0$) is not. A numerical indication of this possibility was also noticed by Barma and Fisher.[12] In addition, Baker[13] found that in the one-dimensional, continuous-spin

Ising model, the cases where $0 < G < \infty$ were in neither the Gaussian not the Ising model universality classes.

Extensive numerical studies of the 2D continuous-spin ϕ^4 model have been carried out. See, for example, Milchev *et al.*[14] and Toral and Chakrabari.[15] However, relatively few published papers focus on the analysis of the universality and crossover from the Gaussian to the Ising limits. Standard, finite-size scaling studies have been made.[14] It was found, near the Ising limit, that the assumption of the Ising class universality was consistent with curve collapsing for systems ranging from 5×5 to 60×60. Near the Gaussian limit, the curve collapsing produces unsatisfactory results for finding conclusive values for the critical exponents. Bruce[16] has simulated the border model, and he does not see inconsistency with the Ising model class universality.

In Section 2 we discuss the model to be studied, and give details on the various types of special cases for which we will give calculational results. In addition, we set out the formulas which are required for the computation of the central charge. We find that the main necessary quantity is the Fourier transform of the energy–energy correlation function in the long-wavelength region.

In Section 3 we describe the hybrid Monte Carlo method which we will use. It is well adapted to be implemented on a massively parallel computer like the CM2. We describe the physical quantities for which we collect data and give a discussion of the possible errors inherent in our procedure.

In Section 4 we describe a test of our methods on the Gaussian model where all the quantities of interest are already known exactly. We find that we obtain quite good results here.

In Section 5 we apply our methods to cases where the spin distribution has a single peak, the border model, and where the spin distribution has a double peak. A good general picture emerges, but we have not been able to carry our computations sufficiently far as yet, even though a very considerable amount of CM2 time has been used, to pin down precisely the questions regarding the correct universality classes appropriate to these particular models. We had (unfortunately) used the Gaussian model estimates for the finite-size effects when we originally laid out our calculations. Those effects are much smaller, as it turns out from a comparison with high-temperature series results for the border model, than is the case in the rest of the work. The departure of one of the authors (X.W.) from Los Alamos has precluded the immediate continuation of this study for different-size lattices. We believe that this continuation would greatly improve our results. In the last section we give a few remarks concerning our results.

2. CONTINUOUS-SPIN ISING MODEL

2.1. The Hamiltonian of the System

The continuous-spin Ising model can be regarded as a one-component, ferromagnetic Ising model where the spins can have values from $-\infty$ to ∞. It can be also viewed as the $:\phi^4:$ Euclidean boson field theory with a lattice cutoff after the quantization of the system.[17,18] The Hamiltonian is defined as

$$H=\sum_{i,j}\left[-K(\phi_{i,j}\phi_{i+1,j}+\phi_{i,j}\phi_{i,j+1})+A\phi_{i,j}^2+G\phi_{i,j}^4\right] \tag{2}$$

where the plane square lattice has been used to discretize space. $\phi_{i,j}$ is the value of the continuous spin at site i, j. Here A and G are the coefficients for the ϕ^2 and ϕ^4 in the potential well. The Hamiltonian (2) has been studied extensively both theoretically and numerically.

All the thermodynamic properties are contained in the partition function, which can be written as

$$Z=\int_{-\infty}^{+\infty}\cdots\int_{-\infty}^{+\infty}e^{-H\{\phi\}}\prod_{i,j}d\phi_{i,j} \tag{3}$$

Aside from an elementary scaling factor for the field variable $\phi_{i,j}$, there are only two independent parameters; we take these to be K and G as in ref. 17. We determine $A(G)$ by the requirement that the second moment of ϕ is normalized to unity, i.e., $\langle\phi_{i,j}^2\rangle_{K=0}=1$, or we determine the value of G by the same requirement when A is zero in the case of the border model.[16,17] The other common way of normalizing ϕ is so that the ϕ^2 and the ϕ^4 terms are proportional to a single parameter.[14] Again there are only two independent parameters.

There are several cases of interest to our study. The simplest case is where the ϕ^4 term is absent, i.e., $A>0$, $G=0$. This case is the Gaussian model. Under the constraint $\langle\phi_{i,j}^2\rangle_{K=0}=1$, A is 1/2. The critical point occurs at $K_c=1/4$ for 2D. Using the notation in ref. 14, we obtain the Hamiltonian for the Gaussian model as

$$H=-\tilde{\beta}\sum_{i,j}(\phi_{i,j}\phi_{i+1,j}+\phi_{i,j}\phi_{i,j+1})+\tilde{\alpha}\sum_{i,j}\frac{1}{2}\phi_{i,j}^2 \tag{4}$$

It is well known that this solvable model has the critical exponents $\alpha=1$ and $\gamma=1$ and a conformal charge of $c=1$, as mentioned above. We will use this model as a test of our method, and then study more general cases.

For the case when $A>0$, $G>0$, both the ϕ^2 term and the ϕ^4 term have the same sign. The potential well has a single minimum. We call it the

single-well case. In the notation of ref. 14, we can also rescale the Hamiltonian into the following form:

$$H = -\tilde{\beta} \sum_{i,j} (\phi_{i,j}\phi_{i+1,j} + \phi_{i,j}\phi_{i,j+1}) + \tilde{\alpha} \sum_{i,j} \left(\frac{1}{2}\phi_{i,j}^2 + \frac{1}{4}\phi_{i,j}^4 \right) \tag{5}$$

The very special case $A = 0$, $G > 0$ lies on the border between the single-well and the double-well model (defined below). There is only one minimum in the potential term, but the curvature is zero at the minimum. Under the constraint $\langle \phi_{i,j}^2 \rangle_{K=0} = 1$, $G \approx 0.11423...$. This case is the so-called border model. In the notation of ref. 14, we may write

$$H = -\tilde{\beta} \sum_{i,j} (\phi_{i,j}\phi_{i+1,j} + \phi_{i,j}\phi_{i,j+1}) + \tilde{\alpha} \sum_{i,j} \frac{1}{4}\phi_{i,j}^4 \tag{6}$$

with $\tilde{\alpha} \approx 0.45692...$.

In one dimension, it can be shown rigorously for this model that a new universality class occurs when $0 < G < \infty$ which is different from the usual Gaussian and Ising universality. As mentioned in the introduction, in two dimensions this model is of great interest. There is no obvious reason why the border model should have the same universality as that of the single-well or the double-well model.

When $A < 0$, $G > 0$, the potential has two degenerate minima. We call this case the double-well model. In the notation of ref. 14,

$$H = -\tilde{\beta} \sum_{i,j} (\phi_{i,j}\phi_{i+1,j} + \phi_{i,j}\phi_{i,j+1}) + \tilde{\alpha} \sum_{i,j} \left(-\frac{1}{2}\phi_{i,j}^2 + \frac{1}{4}\phi_{i,j}^4 \right) \tag{7}$$

In the limit of $\tilde{\alpha} \to \infty$, the double well becomes infinitely deep, and the system effectively reaches the Ising limit.

After scaling ϕ with a scaling factor of ϕ_0, we find the coefficients $\tilde{\alpha}$ and $\tilde{\beta}$ given in Table I in terms of the original A, G. In the following sections we shall examine each individual case to study its critical behavior.

Table I. Rescaling of the Hamiltonian ($K = \phi_0^2 \tilde{\beta}$)

Model	A	G	$\tilde{\alpha}$	ϕ_0
Gaussian	1/2	0	1	1/2
Single-well	0.307756	0.037885	2.5	0.49619
Border	0	0.11423	0.45692	1
Double-well	−1.08080	0.467251	2.5	0.92986

2.2. Computation of Conformal Charge Adopted to Monte Carlo

The usefulness of conformal field theory lies not only at the critical point, but in the vicinity of the critical point as well. From Zamolodchikov's c-theorem, Cardy derived the following explicit formula, which extends the implications of conformal invariance beyond the critical point[8]:

$$c = \lim_{\beta \to \beta_c} \frac{12\pi(\beta_c - \beta)^2}{N^2(2-\alpha)^2} \sum_{\mathbf{r},\mathbf{r}'} |\mathbf{r}-\mathbf{r}'|^2 (\langle \varepsilon_{\mathbf{r}} \varepsilon_{\mathbf{r}'} \rangle - \langle \varepsilon_{\mathbf{r}} \rangle \langle \varepsilon_{\mathbf{r}'} \rangle) \tag{8}$$

where $\varepsilon_{\mathbf{r}}$ represents the interaction energy density at the plane-square lattice site $\mathbf{r}$. Here $|\mathbf{r}-\mathbf{r}'|$ is the distance between $\mathbf{r}$ and $\mathbf{r}'$. (This notation is slightly different from the notation used in ref. 9. The difference is discussed in the latter part of this section.) β is the reduced coupling constant and β_c is its value at the critical point, and α is the critical exponent for specific heat. We use a square lattice (with size $N \times N$) to discretize the space. The energy density $\varepsilon_{\mathbf{r}}$ is chosen to be the sum of four bonds connected to site $\mathbf{r}$, and is given by

$$\varepsilon_{\mathbf{r}} = \frac{1}{2} \sum_{\boldsymbol{\delta}} \phi_{\mathbf{r}} \phi_{\mathbf{r}+\boldsymbol{\delta}} \tag{9}$$

Here the summation over $\boldsymbol{\delta}$ indicates summation over all the neighboring vectors, and the factor of 1/2 comes from the fact that each bond is attached to two lattice sites.

Numerically, it is hard to sum over $\mathbf{r}$, $\mathbf{r}'$ in Eq. (8) directly. One way to reduce the double sum to a single sum is to use the translational invariance of the system and transform $\varepsilon_{\mathbf{r}}$ into Fourier space as

$$\varepsilon_{\boldsymbol{k}} = \frac{1}{2N} \sum_{\mathbf{r},\boldsymbol{\delta}} e^{i\boldsymbol{k}\cdot\mathbf{r}} (\phi_{\mathbf{r}} \phi_{\mathbf{r}+\boldsymbol{\delta}} - \langle \phi_{\mathbf{r}} \phi_{\mathbf{r}+\boldsymbol{\delta}} \rangle) \tag{10}$$

After this transformation, we can then calculate $\langle |\varepsilon_{\boldsymbol{k}}|^2 \rangle$, which is needed to determine the value of the conformal charge. The energy-density correlation function in Fourier space is given by

$$\langle |\varepsilon_{\mathbf{k}}|^2 \rangle = \frac{1}{4N^2} \sum_{\mathbf{r},\mathbf{r}',\boldsymbol{\delta},\boldsymbol{\delta}'} \cos[\mathbf{k}\cdot(\mathbf{r}-\mathbf{r}')] \times (\langle \phi_{\mathbf{r}} \phi_{\mathbf{r}+\boldsymbol{\delta}} \phi_{\mathbf{r}'} \phi_{\mathbf{r}'+\boldsymbol{\delta}'} \rangle - \langle \phi_{\mathbf{r}} \phi_{\mathbf{r}+\boldsymbol{\delta}} \rangle \langle \phi_{\mathbf{r}'} \phi_{\mathbf{r}'+\boldsymbol{\delta}'} \rangle) \tag{11}$$

For small $\mathbf{k}$

$$\cos \mathbf{k}\cdot\mathbf{t} = 1 - \tfrac{1}{2}(k_x^2 t_x^2 + k_y^2 t_y^2 + 2k_x k_y t_x t_y) + \cdots \tag{12}$$

where $\mathbf{t} = \mathbf{r} - \mathbf{r}'$.

The summation over the lattice positions $\mathbf{r}$ will cancel the cross-term by lattice symmetry, so that $\langle|\varepsilon_{\mathbf{k}}|^2\rangle$ is parabolic in $|\mathbf{k}|$ and the rotational symmetry is thus recovered for the long-wavelength region. So we have

$$\langle|\varepsilon_{\mathbf{k}}|^2\rangle = a_0 + a_2|\mathbf{k}|^2 + \cdots \tag{13}$$

where a_0 and a_2 are given by

$$a_0 = \frac{1}{4N^2}\sum_{\mathbf{r},\mathbf{r}',\boldsymbol{\delta},\boldsymbol{\delta}'}(\langle\phi_{\mathbf{r}}\phi_{\mathbf{r}+\boldsymbol{\delta}}\phi_{\mathbf{r}'}\phi_{\mathbf{r}'+\boldsymbol{\delta}'}\rangle - \langle\phi_{\mathbf{r}}\phi_{\mathbf{r}+\boldsymbol{\delta}}\rangle\langle\phi_{\mathbf{r}'}\phi_{\mathbf{r}'+\boldsymbol{\delta}'}\rangle) \tag{14}$$

$$a_2 = -\frac{1}{16N^2}\sum_{\mathbf{r},\mathbf{r}',\boldsymbol{\delta},\boldsymbol{\delta}'}|\mathbf{r}-\mathbf{r}'|^2(\langle\phi_{\mathbf{r}}\phi_{\mathbf{r}+\boldsymbol{\delta}}\phi_{\mathbf{r}'}\phi_{\mathbf{r}'+\boldsymbol{\delta}'}\rangle - \langle\phi_{\mathbf{r}}\phi_{\mathbf{r}+\boldsymbol{\delta}}\rangle\langle\phi_{\mathbf{r}'}\phi_{\mathbf{r}'+\boldsymbol{\delta}'}\rangle) \tag{15}$$

The definition of the energy density and the subsequent derivations are slightly different from the definition used in ref. 9, where $\varepsilon_{\mathbf{r}}$ represent the interaction energy density at the *bond* of the square lattice instead of the sites. In that case, $\varepsilon_{\mathbf{k}}$ was given by

$$\varepsilon_{\mathbf{k}} = \frac{1}{2N}\sum_{\mathbf{r},\boldsymbol{\delta}}\left\{\exp\left[i\mathbf{k}\cdot\left(\mathbf{r}+\frac{1}{2}\boldsymbol{\delta}\right)\right]\right\}(\phi_{\mathbf{r}}\phi_{\mathbf{r}+\boldsymbol{\delta}} - \langle\phi_{\mathbf{r}}\phi_{\mathbf{r}+\boldsymbol{\delta}}\rangle) \tag{16}$$

which differs from the definition in this paper by the small phase factor $\exp(i\mathbf{k}\cdot\boldsymbol{\delta}/2)$. Consequently,

$$\langle|\varepsilon_{\mathbf{k}}|^2\rangle = \frac{1}{4N^2}\sum_{\mathbf{r},\mathbf{r}',\boldsymbol{\delta},\boldsymbol{\delta}'}\cos\left[\mathbf{k}\cdot\left(\mathbf{r}+\frac{1}{2}\boldsymbol{\delta}-\mathbf{r}'-\frac{1}{2}\boldsymbol{\delta}'\right)\right] \tag{17}$$

$$\times(\langle\phi_{\mathbf{r}}\phi_{\mathbf{r}+\boldsymbol{\delta}}\phi_{\mathbf{r}'}\phi_{\mathbf{r}'+\boldsymbol{\delta}'}\rangle - \langle\phi_{\mathbf{r}}\phi_{\mathbf{r}+\boldsymbol{\delta}}\rangle\langle\phi_{\mathbf{r}'}\phi_{\mathbf{r}'+\boldsymbol{\delta}'}\rangle) \tag{18}$$

The result for a_0 is identical to Eq. (14), and that for a_2 differs from Eq. (15) by the addition of the extra term

$$\frac{1}{16N^2}\sum_{\mathbf{r},\mathbf{r}',\boldsymbol{\delta},\boldsymbol{\delta}'}|\boldsymbol{\delta}-\boldsymbol{\delta}'|^2(\langle\phi_{\mathbf{r}}\phi_{\mathbf{r}+\boldsymbol{\delta}}\phi_{\mathbf{r}'}\phi_{\mathbf{r}'+\boldsymbol{\delta}'}\rangle - \langle\phi_{\mathbf{r}}\phi_{\mathbf{r}+\boldsymbol{\delta}}\rangle\langle\phi_{\mathbf{r}'}\phi_{\mathbf{r}'+\boldsymbol{\delta}'}\rangle) \tag{19}$$

The odd terms in the $\boldsymbol{\delta}$'s vanish by lattice symmetry. The term in Eq. (19) is small relative to that in Eq. (15) for a large lattice near the critical point. [The ratio is approximately a factor of $(|\boldsymbol{\delta}|/\xi)^2$, where ξ is the correlation length of the system.] Equation (13) is only approximate in a Monte Carlo simulation, however, as the cross-terms vanish only like the Monte Carlo errors.

The specific heat of the system is given by

$$C_v = \frac{1}{N^2\beta^2}\left[\left\langle\left(\sum_{\mathbf{r}}\varepsilon_{\mathbf{r}}\right)^2\right\rangle - \left\langle\left(\sum_{\mathbf{r}}\varepsilon_{\mathbf{r}}\right)\right\rangle^2\right] \tag{20}$$

where $\mathbf{r}$ runs over the sites of the system. From Eq. (14) we have that

$$C_v = \frac{a_0}{\beta^2} \tag{21}$$

The critical exponent α can be found by analyzing the specific heat C_v near the critical point. From Eqs. (8) and (15) we have the formula for conformal charge

$$c = \lim_{\beta \to \beta_c} \frac{48\pi}{(2-\alpha)^2} a_2 (\beta - \beta_c)^2 \tag{22}$$

This formula can also be derived directly from (8) and (11) by noting that

$$\nabla_{\mathbf{k}}^2 \langle |\varepsilon_{\mathbf{k}}|^2 \rangle_{\mathbf{k}=0} = \sum_{\mathbf{r},\mathbf{r}'} |\mathbf{r} - \mathbf{r}'|^2 (\langle \varepsilon_{\mathbf{r}} \varepsilon_{\mathbf{r}'} \rangle - \langle \varepsilon_{\mathbf{r}} \rangle \langle \varepsilon_{\mathbf{r}'} \rangle) \tag{23}$$

where $\mathbf{r}$ and $\mathbf{r}'$ run over the sites of the lattice.

In practice, we only need to calculate the spectrum of the local energy–energy correlation $\langle |\varepsilon_{\mathbf{k}}|^2 \rangle$ by Monte Carlo sampling of the ϕ field and to transform it to Fourier space. Then, we need to find the curvature and height at $\mathbf{k} = 0$. This determination can be done by fitting the 2D $\langle |\varepsilon_{\mathbf{k}}|^2 \rangle$ surface with a high-order polynomial. (Typically we have chosen eighth order for our studies.) The fitting coefficients give $a_0, a_2, \ldots$. Only the first two coefficients are needed for our purposes in this paper. A more detailed discussion of this procedure is given in Sections 3 and 4.

3. MONTE CARLO SCHEME

3.1. Hybrid Algorithm

To calculate the physical observables, we need to sample the configuration $\phi_{i,j}$ under the Boltzmann weights appearing in the partition function of the system. The sampling process is usually done by employing the conventional Metropolis algorithm where the sampled configuration $\phi_{i,j}$ is randomly chosen from the configurational space, or by employing the Langevin algorithm in which the sampled configurations are obtained by diffusive trajectories.

We use here the hybrid Monte Carlo algorithm,[19] which is a combination of a molecular dynamics algorithm and the Metropolis algorithm. Within this algorithm, each $\phi_{i,j}$ is regarded as the coordinate of an "atom" with an assigned *pseudomass* m. In this way, there is an associated

pseudomomentum $\pi_{i,j}$ for each "atom" at position $\phi_{i,j}$. The *pseudo-Hamiltonian* of the new system can be written as

$$H_{\text{pse}}\{\phi, \pi\} = \sum_{i,j} \frac{\pi_{i,j}^2}{2m} + H\{\phi\} \tag{24}$$

We can have well-defined Hamiltonian dynamics under the pseudo-Hamiltonian with a fictitious *pseudotime* t. The equations of motion are

$$\frac{d\phi_{i,j}}{dt} = \frac{\partial H_{\text{pse}}}{\partial \pi_{i,j}}, \qquad \frac{d\pi_{i,j}}{dt} = -\frac{\partial H_{\text{pse}}}{\partial \phi_{i,j}} \tag{25}$$

The partition function of the pseudosystem is then given by

$$Z_{\text{pse}} = \int \prod_{i,j} d\phi_{i,j}\, d\pi_{i,j} e^{-H_{\text{pse}}\{\phi,\pi\}}$$

The integration over $\pi_{i,j}$ is Gaussian and can be carried out easily. It gives rise to $Z_{\text{pse}} = (2\pi m)^{NL/2} Z$, where Z is defined in Eq. (3). The pseudo partition function thus differs from the true partition function only by a constant factor. The physical observables measured in this pseudosystem (under the Boltzmann weight for the pseudosystem) are thus the same as would be measured in the original system.

The sampling of the system is achieved by the following procedure. We initialize all the $\phi_{i,j}$ to be zero. Then we repeat as required the following set of actions: First, we generate the $\pi_{i,j}$ according to a Gaussian distribution. Second, we measure the value of the pseudo-Hamiltonian $H_{\text{pse}}^{\text{bef}}$. Third, we set the $\phi_{i,j}$ to be their last accepted values (which on the first pass are those given above). Fourth, we let the $\phi_{i,j}$, $\pi_{i,j}$ evolve under Eq. (25) in pseudotime t. Fifth, after pseudotime T has elapsed, we measure the value of the pseudo-Hamiltonian $H_{\text{pse}}^{\text{aft}}$. Sixth, we accept the newly computed $\phi_{i,j}$ with probability $\min[1, \exp\{-(H_{\text{pse}}^{\text{aft}} - H_{\text{pse}}^{\text{bef}})\}]$. Finally, we measure the physical observables (after the thermalization of the system is achieved). We then, as indicated above, repeat this process as required.

The value of T is typically, for our studies, chosen to be 3–5 times the characteristic time of each individual oscillator. We expect that the pseudo-Hamiltonian $H_{\text{pse}}^{\text{aft}}$ after the evolution for pseudotime T deviates from its starting value. This small but finite error may heat up or cool down the system, and results in an inaccuracy in terms of the temperature control, because we use fairly large integration steps. Fortunately, this integration error can be completely canceled by combination with the Metropolis algorithm at step 6. It can be shown that the above procedure properly leads to the correct thermalization of the original system.[19] After the

thermalization of the system, we then measure the physical quantities for every sampled state until the statistical errors are small enough. The typical number of measurements we chose for a 128×128 size system ranged from 100,000 to 400,000.

At or near the critical point, the configuration of $\phi_{i,j}$ primarily consists of domain walls. By evolving the system in phase space according to Eq. (25), the domain walls can propagate freely in space instead of encountering large energy barriers. The propagation is essentially linear in t, in contrast to the diffusive motion sampled by the simple Metropolis or Langevin algorithms, which go only like the square root in t. The sampling of the configurational space is thus much faster, and results in less correlation among the consecutive measurements. In addition, this algorithm is naturally suitable for parallelization on massively parallel machines such as the Connection Machine.

3.2. Measurements

Any physical quantity can be measured in term of the sampled $\phi_{i,j}$ configurations. The ensemble average of a physical quantity A is given by

$$\langle A \rangle = \frac{1}{M} \sum_{m=1}^{M} A\{\phi_i\} \tag{26}$$

where M is the number of sweeps (repetitions). The physical quantities of interest include the energy of the system

$$E(\beta) = \frac{1}{N^2} \langle H \rangle \tag{27}$$

and the bond energy

$$\Xi(\beta) = \frac{1}{N^2} \left\langle \sum_{\mathbf{r}} \varepsilon_{\mathbf{r}} \right\rangle \tag{28}$$

The conventional definition of the order parameter X is

$$X(\beta) = \frac{1}{N^2} \left\langle \sum_{i,j}^{L,N} \phi_{i,j} \right\rangle \tag{29}$$

which is appropriate when there is a small magnetic field. For Monte Carlo simulations in zero field, we take

$$X_{\mathrm{MC}}(\beta) = \frac{1}{N^2} \left\langle \left| \sum_{i,j}^{L,N} \phi_{i,j} \right| \right\rangle \tag{30}$$

when $\beta > \beta_c$. The absolute sign here allows us to compute the spontaneous magnetization properly in zero field for the bimodal distribution of X expected when $\beta > \beta_c$. The susceptibility χ of the system is

$$\chi(\beta) = N^2(\langle X^2 \rangle - \langle X \rangle^2) \tag{31}$$

where X is defined above. This expression does not lead to the thermodynamically desired result on the first-order phase transitional line of zero magnetic field for $\beta > \beta_c$, so the commonly used expedient is to measure the susceptibility of the system with X replaced by X_{MC} in Eq. (31).[14] However, (31) is correct on the high-temperature side $\beta < \beta_c$ where $\langle X \rangle = 0$. Most of our studies hereafter are on the high-temperature side of the critical point and the definition (31) is used unless specified otherwise.

The specific heat is given by Eq. (21). The critical exponents α and γ can be found by plotting C_v and χ versus $\beta - \beta_c$. The most important quantity is the energy–energy correlation function $\langle |\varepsilon(\mathbf{k})|^2 \rangle$, which gives the specific heat [and hence the critical exponent α and the conformal charge; see Eqs. (21) and (22)].

3.3. Discussion of Possible Errors

There are many possible sources of error, which can be classified as the statistical errors and the systematic errors. The major statistical error is due to the finite number of states sampled and measured. We typically take 100,000–400,000 measurements for the physical quantities we studied in order to achieve reasonable statistics. Our simulations show that near the Gaussian limit, the statistical error is less severe than near the Ising limit.

There are several sources of systematic errors. One is the finite-size effect. We limit our study to a system of size 128×128. The finite size of the system will suppress the divergence of the specific heat and the susceptibility at the critical point and will reduce the divergent peaks to finite heights. In addition, we expect that the peaks' position will not in general coincide with β_c. So there is a narrow region within which the scaling behavior differs significantly from that of an infinite system. This region needs be excluded to obtain the appropriate exponents and the conformal charge. For the size of 128×128, we generally discard data from within about 1% of the critical point.

Another systematic error involves the determination of the critical point β_c from the MC simulations. The accuracy of β_c can affect the accuracy of exponents and the conformal charge obtained. In practice we determine β_c by running several MC simulations near β_c and locate the

peak positions of C_v and χ. In this way a very good estimate of β_c can be obtained, with more than three-decimal accuracy, for our 128×128 system. Finite-size scaling theory predicts that the fractional shift of the peak in say, C_v, from β_c is proportional to $N^{-1/\nu}$. For the case of the Ising model, Ferdinand[20] gives

$$\frac{\beta_c}{\beta_{c,N}} \approx 1 + \frac{0.35}{N} \tag{32}$$

for periodic boundary conditions. Here, β_c and $\beta_{c,N}$ are the critical points for the infinite-size system and size-N system, respectively. For $N = 128$, we have about 1.0027 for this ratio, or 3 parts in 10^3. For the Gaussian case the correction is much smaller, as $\nu = 1/2$. Estimates for the critical indices can be in error by a much larger amount, as can be seen by considering the case of extrapolation from $\beta/\beta_c = 0.99$ (to reduce higher corrections) with the peak-location–critical-temperature difference as quoted above for the Ising model.

Far away from the critical point in the high-$\mathbf{k}$ region, we no longer have the rotational symmetry around the $\mathbf{k} = 0$ point. To fit the $\langle |\varepsilon(\mathbf{k})|^2 \rangle$ to obtain a_2, in principle, only the information in the vicinity of $\mathbf{k} = 0$ is needed. However, an overly small area may not give a meaningful fit of the height and the curvature at the peak of $\langle |\varepsilon(\mathbf{k})|^2 \rangle$, so in practice, a judgement has to made to choose an appropriate area to fit to find a_2.

The fitting procedures for the exponents and conformal charge also introduce systematic errors, especially for finding the curvature of $\langle |\varepsilon_{\mathbf{k}}|^2 \rangle$. For that purpose only a_0 and a_2 are used to find the specific heat and the conformal charge. However, we choose the eighth-order polynomial in our fitting procedure, i.e., find the coefficients for the terms $|\mathbf{k}|^2$, $|\mathbf{k}|^4$, $|\mathbf{k}|^6$, and $|\mathbf{k}|^8$. The eighth order was chosen only for the purpose of being able to capture the nonquadratic effects near $|\mathbf{k}| = 0$, while at the same time maintaining the simplicity of the fitted form and the fitting procedure. The cross-terms such as the $k_x k_y$ term are canceled because of the symmetry of the crystal up to second order; however, the higher-order cross-terms are, in general, not all canceled. Our fitting procedure, which does not take into account the higher-order cross-terms, suppresses the effects of these terms. To emphasize properly the region near $\mathbf{k} = 0$, we arbitrarily chose a weighting factor of $\sigma \propto \exp(-\text{const} \cdot |\mathbf{k}|^2/\Delta\beta)$, where $\Delta\beta = |\beta - \beta_c|$ and the constant const ≈ 0.01. This choice is a fairly reasonable one for our fitting procedure to compromise between the large-$\mathbf{k}$ and the small-$\mathbf{k}$ regions for $0.01 < \Delta\beta < 0.1$.

4. TEST OF OUR METHOD ON THE GAUSSIAN MODEL

We would like to test quantitatively our method of studying the conformal charge and at the same time to study quantitatively the different aspects of the errors discussed in the last section. The solvable Gaussian model as the limit of ϕ^4 models where $G \to 0$ provides us with a good test. Although a successful test does not necessarily imply that our techniques work for all other cases, it nonetheless can provide a significant amount of insight.

The Gaussian model Hamiltonian is given by Eq. (4). The spin–spin correlation function for a finite-size system with periodic boundary conditions is given by

$$\langle \phi_{\mathbf{r}} \phi_{\mathbf{r}'} \rangle = \frac{1}{2N^2} \sum_{\mathbf{k}} \frac{\cos[\mathbf{k} \cdot (\mathbf{r} - \mathbf{r}')]}{A - K(\cos k_x + \cos k_y)} \tag{33}$$

where $\mathbf{k}$ is in units such that the lattice spacing is unity. By using the identity

$$\begin{aligned} &\langle \phi_{\mathbf{r}} \phi_{\mathbf{r}+\boldsymbol{\delta}} \phi_{\mathbf{r}'} \phi_{\mathbf{r}'+\boldsymbol{\delta}'} \rangle - \langle \phi_{\mathbf{r}} \phi_{\mathbf{r}+\boldsymbol{\delta}} \rangle \langle \phi_{\mathbf{r}'} \phi_{\mathbf{r}'+\boldsymbol{\delta}'} \rangle \\ &\quad = \langle \phi_{\mathbf{r}} \phi_{\mathbf{r}'} \rangle \langle \phi_{\mathbf{r}+\boldsymbol{\delta}} \phi_{\mathbf{r}'+\boldsymbol{\delta}'} \rangle + \langle \phi_{\mathbf{r}+\boldsymbol{\delta}} \phi_{\mathbf{r}'} \rangle \langle \phi_{\mathbf{r}} \phi_{\mathbf{r}'+\boldsymbol{\delta}'} \rangle \end{aligned} \tag{34}$$

which holds for the Gaussian model, it is straightforward to show from Eqs. (9) and (33) by performing the sums over $\mathbf{r}$, $\mathbf{r}'$, $\boldsymbol{\delta}$, and $\boldsymbol{\delta}'$ that the energy–energy correlation for a finite-size square lattice is

$$\langle |\varepsilon(\mathbf{k})|^2 \rangle = \frac{1}{4N^2} \sum_{\mathbf{q}} \frac{\begin{pmatrix} (\cos q_x + \cos q_y)^2 + [\cos(k_x - q_x) \\ + \cos(k_y - q_y)](\cos q_x + \cos q_y) \end{pmatrix}}{\begin{pmatrix} \{A - K[\cos(k_x - q_x) + \cos(k_y - q_y)]\} \\ \times [A - K(\cos q_x + \cos q_y)] \end{pmatrix}} \tag{35}$$

This formula can be calculated by numerical evaluation of the above summation. Thus one can compare it with the results of Monte Carlo (MC) simulation. In general, the correlations reflect the square lattice structure; however, the rotational symmetry should be seen for small enough $|\mathbf{k}|$.

The statistical error is one of the major errors of MC simulations. It is hard to estimate this error objectively. The error estimate from the binning analysis usually underestimates the true error. To see this error for

the Gaussian model, in Fig. 1 we plot the MC result against the analytical calculation from Eq. (35). The difference between these two is quite small, the biggest relative deviation from the theoretical calculation is 0.8%. As the temperature β gets closer to β_c, a peak emerges from the $\mathbf{k}=0$ region in the energy–energy correlation $\langle|\varepsilon(\mathbf{k})|^2\rangle$. From Eqs. (22) and (21), it can be seen that the height of the emerging peak determines the specific heat of the system, and the curvature at the tip of the peak determines the conformal charge of the system.

The specific heat of the system can be obtained as in Eq. (21). We plot our result for C_v in Fig. 2. As we approach closer to the critical point, the finite-size effects start to play a very important role. The C_v value is smaller than for the infinite-size system within this region. Our experience here

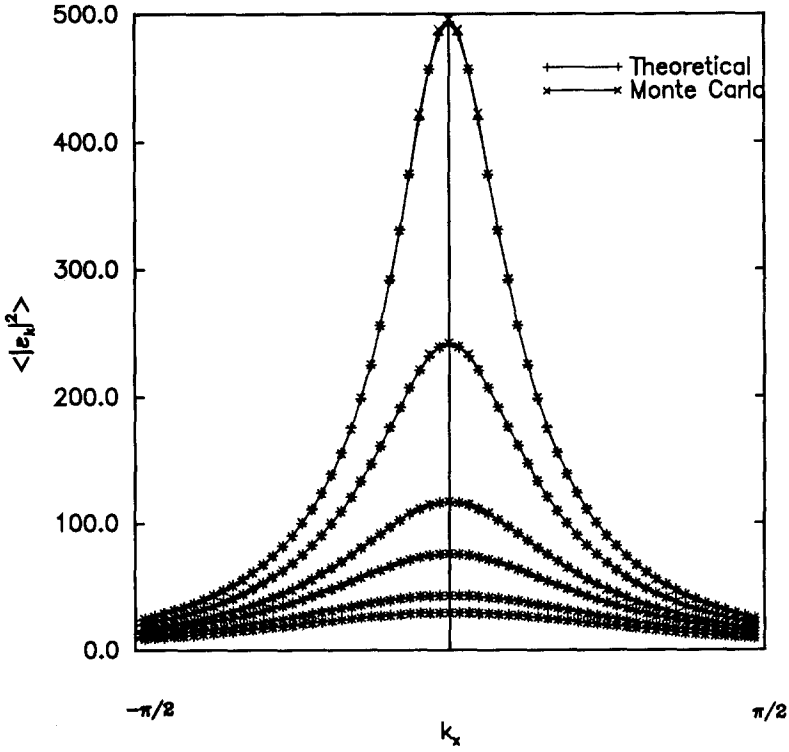

Fig. 1. The energy–energy correlation function $\langle|\varepsilon_{\mathbf{k}}|^2\rangle$ of the Gaussian model obtained from theoretical calculation of a system of 128×128 sites and the MC calculation for the same size system (no fitting procedure is used here). The relatively small difference that can be seen from the plot indicates the small statistical error from the MC sampling. The temperatures for the curves are, in order of decreasing height, $\beta/\beta_c=0.995$, 0.99, 0.98, 0.97, 0.95, and 0.93, respectively.

shows that within a region of $(\beta_c - \beta)/\beta_c$ from 0.01 to 0.10, we are essentially in a good scaling region, for our system is 128×128. This region is wide enough for the Gaussian model to extract the critical exponent α by plotting the C_v in logarithmic scale and fitting the plot to a straight line with a standard χ^2 fitting routine. The slope is found to be $\alpha \approx 1.08$ from the theoretical formula, and $\alpha \approx 1.09$ from MC simulation. Both are higher than the expected value of 1.00. The fitting error is only about 1% from our fitting procedure. This value underestimates the true error significantly, for both theoretical results and the MC simulations. This error is likely to have originated from the systematic effects caused by a combination of finite-size effects and the effect of the region over which we chose to fit our lines ($0.01 < \Delta\beta < 0.1$). This latter effect can be seen from a small curvature in the downward direction, where we do see the slope approaching 1 as $\beta \to \beta_c$. The theoretical expression for the susceptibility in the Gaussian

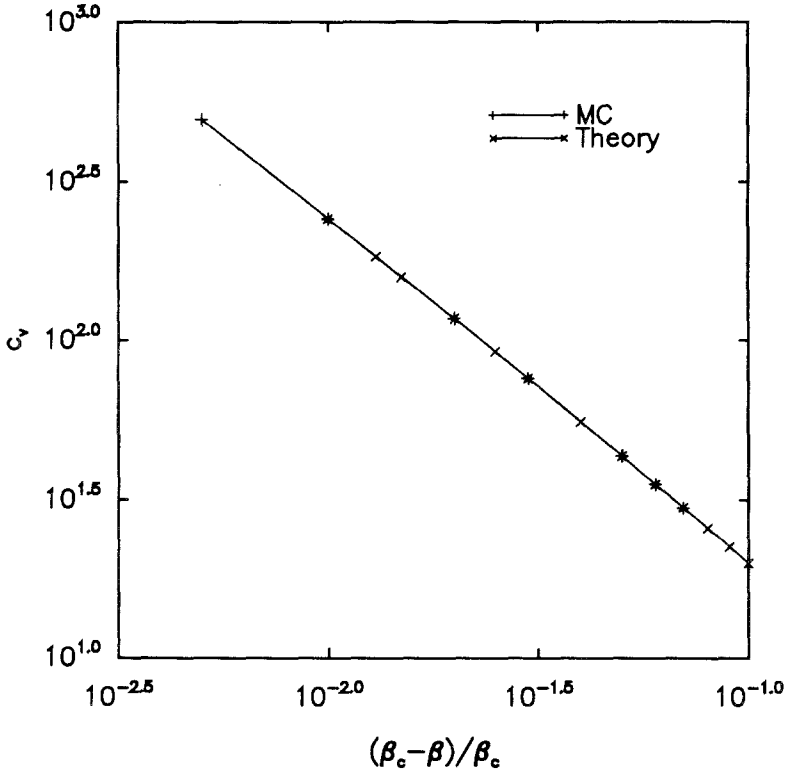

Fig. 2. The specific heat C_v of the Gaussian model obtained from MC calculation for the 128×128 sites system. Nearly straight line in log-log plot indicates the power-law in specific heat.

model can be easily calculated from Eq. (33) by summing over $\mathbf{r}$ and $\mathbf{r}'$ and combining with Eq. (31) and setting $\langle X \rangle = 0$, which gives

$$\chi = \frac{1}{2(A - 2K)} \tag{36}$$

The susceptibility is obtained by Eq. (31). Both the analytical results and the MC results are plotted in Fig. 3. The fairly straight line indicates that, within the same region as plotted for C_v, the susceptibility of is also effectively in the good scaling region. Similar to obtaining α, the critical exponent γ can be obtained in the same way, which gives $\gamma \approx 1.01$, about 1% deviation from the true value of 1.00. The fitting error for γ is 0.005, which again underestimates the error.

The calculation of the conformal charge c depends on the value of α, as can be seen from Eq. (22). From the fitting result of $\langle |\varepsilon(\mathbf{k})|^2 \rangle$ to find a_2, we can obtain $c(2-\alpha)^2$. In Fig. 4, we show the results of our calculation for

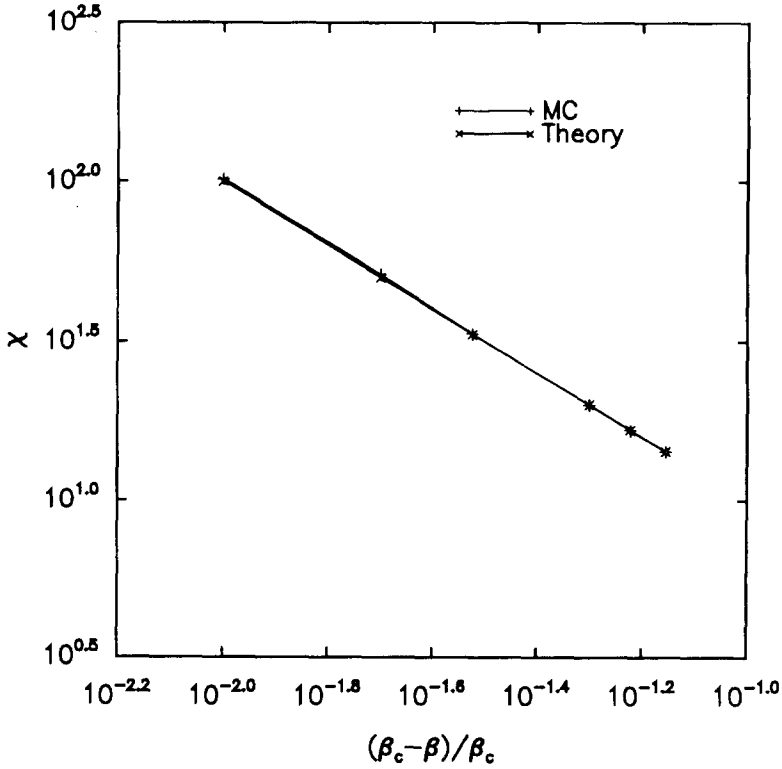

Fig. 3. The susceptibility χ for the Gaussian model obtained from theoretical calculation from Eq. (36) and MC calculation for the 128×128 site system. The two lines essentially overlap each other in the plot.

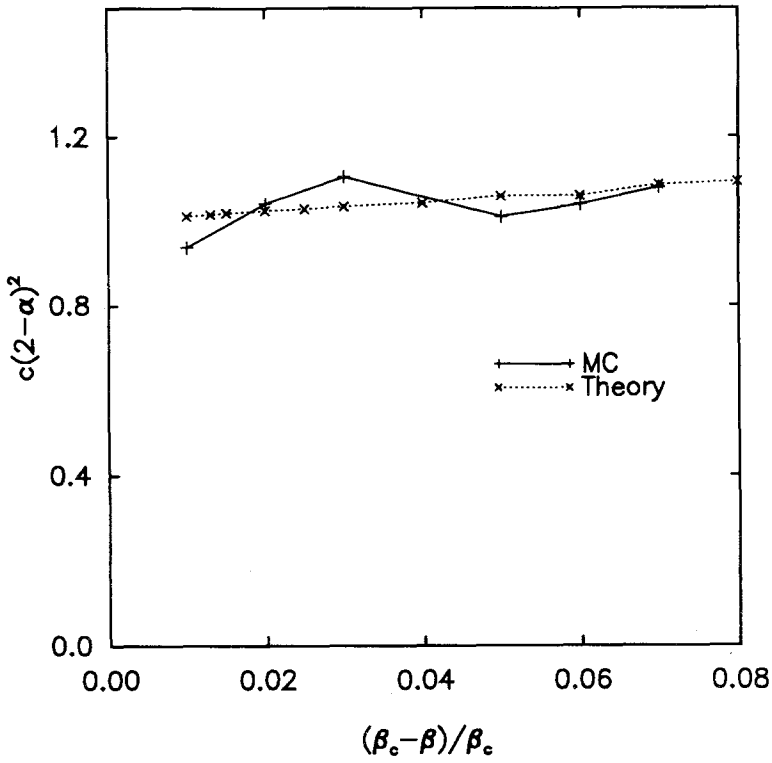

Fig. 4. The comparison of the conformal charge of the Gaussian model obtained from theoretical calculation of the 128×128 site system and the MC calculation for the same size system. The fitting to obtain a_2 as in Eq. (13) is done with eighth-order polynomial fitting with rotational symmetry around $\mathbf{k}=0$.

$c(2-\alpha)^2$. Visually, the analytic data look like a straight line in terms of $\Delta\beta$, and so we have fit the MC data to a straight line and extrapolated to $\Delta\beta=0$ to find the value of $c(2-\alpha)^2$. We thus obtain the result of $c(2-\alpha)^2 \approx 1.004 \pm 0.005$ from our theoretical formula and $c(2-\alpha)^2 \approx 0.999 \pm 0.07$ from our MC calculations. The error bars are the fitting error alone. It is interesting to notice that the results of $c(2-\alpha)^2$ for both theoretical and MC data are considerably less affected by the systematic effects than were α and γ. It is hoped that this nice property still persists for the rest of the cases where no exact solution is available.

5. SINGLE-WELL, BORDER, AND DOUBLE-WELL MODELS

The real interest in the continuous-spin ϕ^4 model is for cases where the exact solution of the system is not available. We will focus our attention on

the cases of the single-well model, the border model, and the double-well model as discussed in Section 2. In particular, we are only going to choose one parameter set for each case as a representative of that case rather than carrying out an exhaustive study of the whole parameter space.

The single-well case is an interesting one since it represents the effects of the nonlinear ϕ^4 term, which will likely modify the critical behavior of the Gaussian model greatly. This region of parameter space has been studied by the technique of finite-size scaling. It has been shown that the curve-collapsing process of finite-size scaling produces a poor "universal" curve.[14] An "effective" critical exponent of $\nu \approx 0.8$ was obtained in this case to describe approximately the critical behavior in this region. We choose $\tilde{\alpha} = 2.5$ for this model, which is closer to the displacive limit compared with ref. 14. For the border model, except for the overall scaling factor for $\phi_{i,j}$, no further parameters can be changed. We study the border model as given in Eq. (6). When the potential term has the shape of a

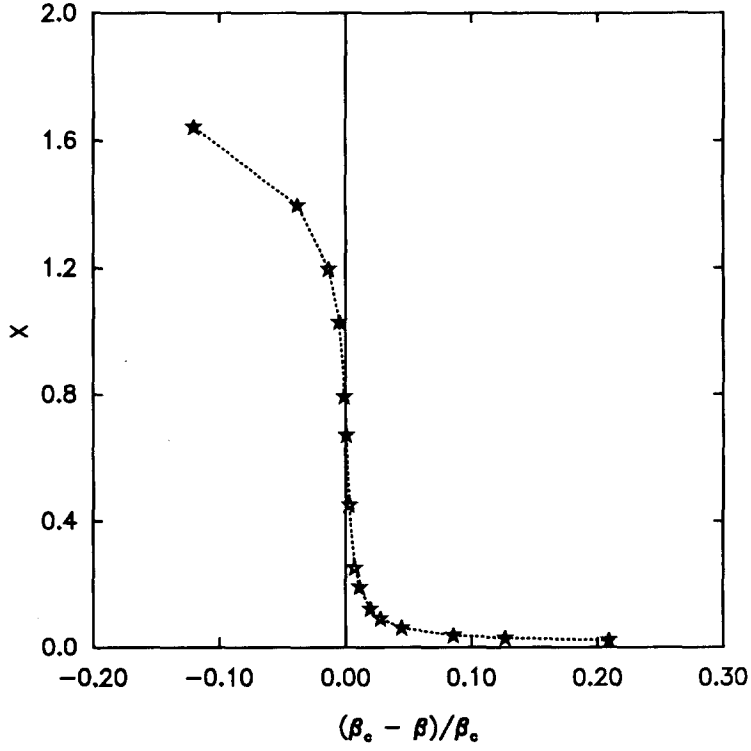

Fig. 5. The order parameter for the single-well model. The size of the system is 128×128. The critical temperature is about $K_c \approx 0.2989$.

double well as in (7), we choose the point in the parameter space which coincides with the simulation in ref. 14 where $\tilde{\alpha} = 2.5$, so that comparison with previous work can be made easily. For these parameters, it has been shown in ref. 14 that the finite scaling relations can be applied to obtain the curve collapsing for different sizes of the system. The behavior was found to be consistent with the Ising model universality assumption.

For convenience in the comparison of the different models, we here choose the normalization so that $\langle \phi_{i,j}^2 \rangle_{K=0} = 1$ for all of the models, so that far away from the criticality, all C_v will behave the same. We tabulate the parameters in Table I.

Most of our studies are done with 128×128 systems. We illustrate the results in detail for the single-well model first. Qualitatively, the behaviors of the single-well model, the border model, and double-well model are similar. In the latter part of this section, we summarize our results for all the models studied.

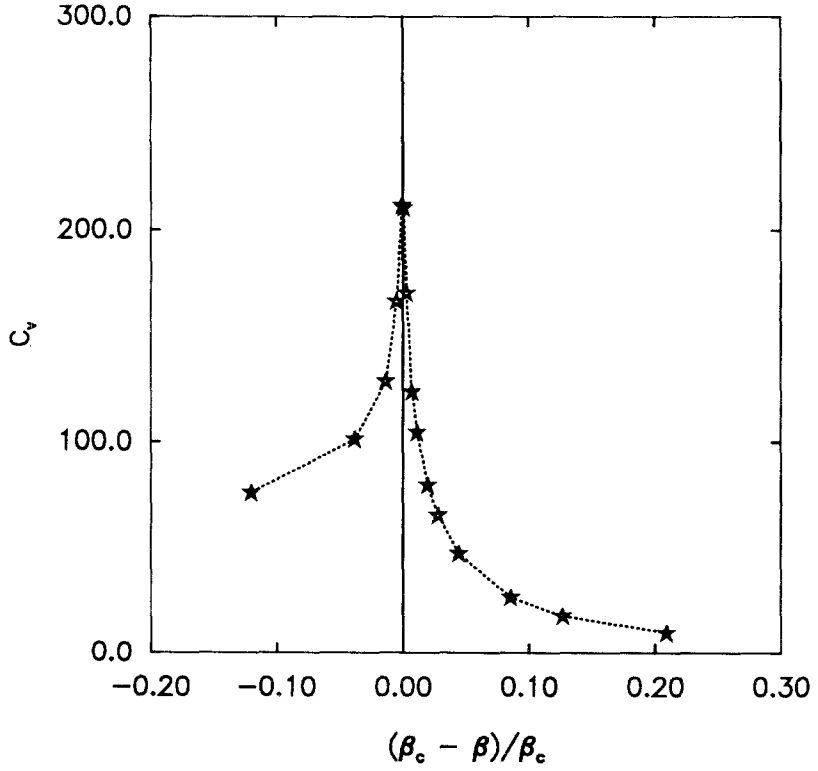

Fig. 6. The specific heat for the single-well model. The size of the system is 128×128. The critical temperature is about $K_c \approx 0.2989$.

The magnetization X_{MC}, specific heat C_v, and the susceptibility χ of the single-well model are shown in Figs. 5–7. The apparent divergent peak appears near $K_c \approx 0.2989$ after normalizing $\langle \phi_{i,j}^2 \rangle = 1$ ($\tilde{\beta}_c \approx 1.2142$ before the normalization). This β_c is obtained by the simple extrapolation near the critical point as explained in Section 3.3.

When the temperature is close to the critical temperature, we study the energy–energy correlation $\langle |\varepsilon_{\mathbf{k}}|^2 \rangle$ of the model. As the critical temperature is approached, a divergent peak emerges near the $\mathbf{k} = 0$ position. We illustrate this behavior in Figs. 8 and 9. We show $\langle |\varepsilon_{\mathbf{k}}|^2 \rangle$ for the single-well model. Similarly, we have carried out simulations for the border model and double-well model with the same size of 128×128. It is noticeable that the amount of the statistical error present for our simulations gets increasingly larger as we approach the Ising side. So, relatively longer runs were made in our simulations of these systems to compensate for some of those effects.

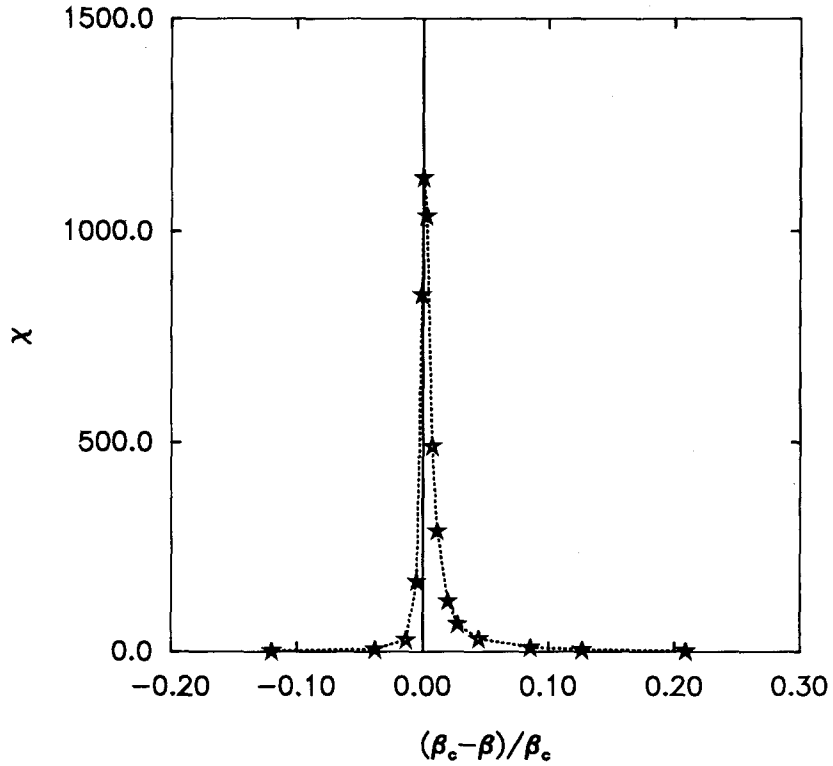

Fig. 7. The susceptibility plot for the single-well model. The size of the system is 128×128. The critical temperature is about $K_c \approx 0.2989$.

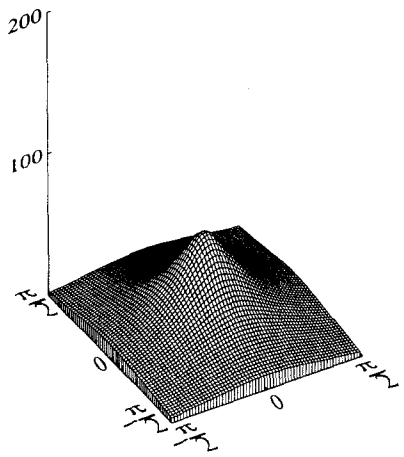

Fig. 8. The energy–energy correlation function for the single-well model, at temperature $K = 0.2905$ (or $\tilde{\beta} = 1.1800$) with 100,000 measurement taken.

(The number of measurements for the border model and double-well model range from 200,000 to 400,000 in the data given below.) For the border model, the critical temperature is found to be near $K_c \approx 0.3288$ (or $\tilde{\beta}_c \approx 0.3288$). This value is considerably different from the series analysis value of Baker and Johnson,[21] who give $K_c \approx 0.3300$, and the difference is in line with the predicted finite-size effect discussed in Section 3.3 for the Ising model. For the double-well model the specific heat and susceptibility

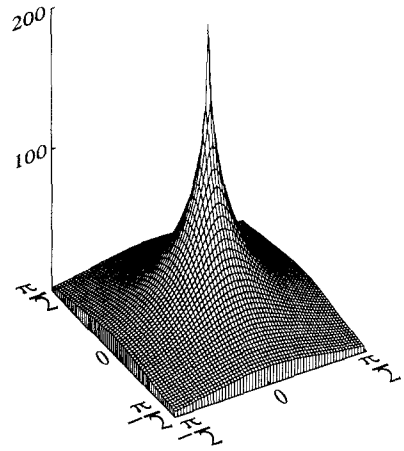

Fig. 9. The energy–energy correlation function for the single-well model, at temperature $K = 0.2986$ (or $\tilde{\beta} = 1.2130$) with 100,000 measurement taken.

peaked at $K_c \approx 0.3722$ (or $\beta_c \approx 0.4305$; this value is slightly different from ref. 14, which has a value of $\tilde{\beta} \approx 0.428$).

Because of the finite-size effects, near β_c, the divergence in C_v and χ for an infinite system is rounded. Within a small region near K_c (say, $\Delta\beta < 0.01$ for 128×128 systems), we expect the physical quantities calculated from the finite-size system, such as C_v, χ, etc., to differ from their true values for an infinite system. As we just mentioned, we expect that the critical temperature obtained from the finite-size system should differ from the true critical temperature for the infinite system. So we cannot take too seriously the data within this region.

In Fig. 10 we plot the specific heat with respect to the relative temperature from β_c. The nearly straight lines in the log-linear plot indicate that the leading term in the divergence of the specific heat is not inconsis-

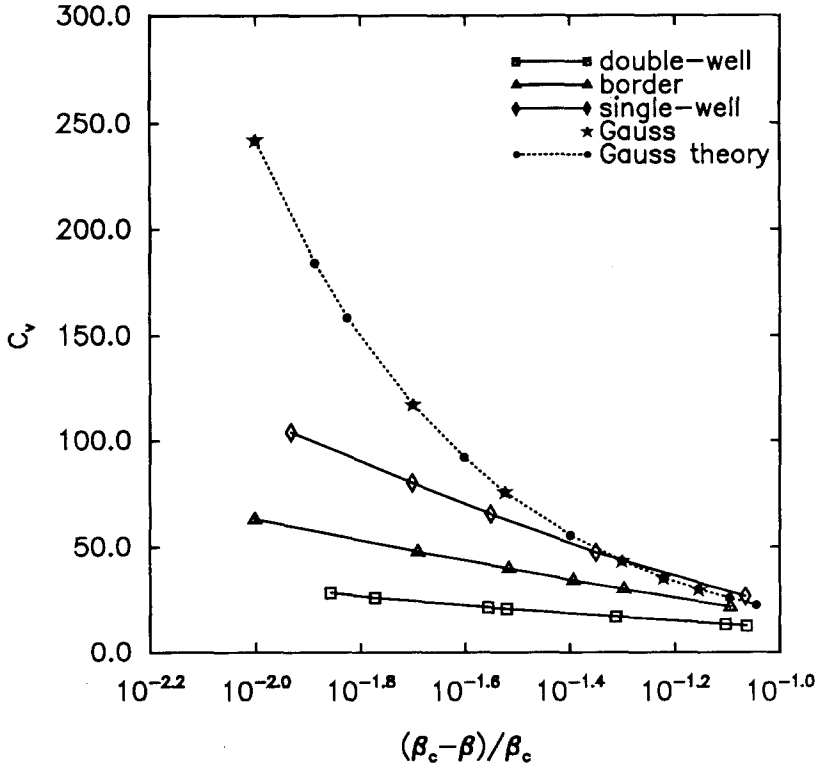

Fig. 10. Specific heat C_v for the different models studied. Notice that the plot is on a log-linear scale. The nearly straight lines indicate the logarithmic divergence for the single-well model, the border model, and the double-well model, which is significantly different from the power-law behavior of the Gaussian model.

tent with logarithmic behavior as is the case for the known Ising model. It is, however, noticeable beyond the uncertainty of statistical error that the C_v plot is not really a straight line. This observation may be due to many possible factors. In Fig. 11, we plot the susceptibility of the models we have studied so far. With the log-log scale of the plot, a nearly straight line indicates a power-law behavior of the susceptibilities (although the amount of statistical fluctuation for the double-well model is still noticeably strong even with 300,000–400,000 measurements taken). The slopes of the lines for the single-well model, the border model, and the double-well model are significantly different from the slope for the Gaussian model, indicating different critical exponents. We calculate the slope of each line by fitting the plot to straight lines with a standard χ^2 fitting routine. The fitted results are listed in Table II. The conformal charges are calculated from the results

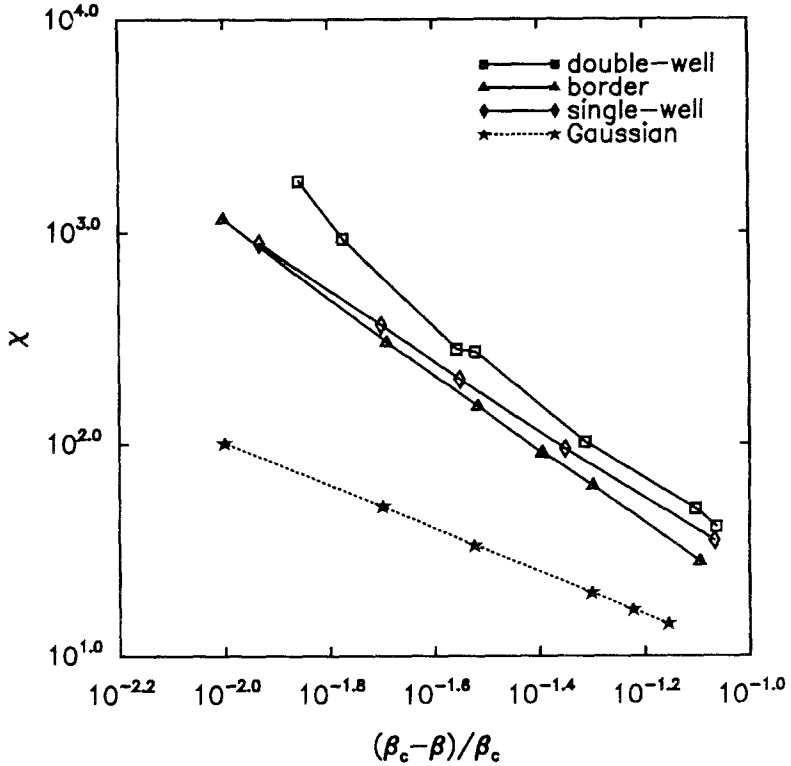

Fig. 11. Susceptibility χ for the different models studied, with the definition as in Eq. (31). Notice that the plot is on a log-log scale. The nearly straight lines indicate the power-law divergence for the single-well model, the border model, and the double-well model. The slope is significantly different from the slope of the Gaussian model.

Table II. Fitted γ and $c(2-\alpha)^2$ for Different Models[a]

	Gauss (theory)	Gauss (MC)	Single-well	Border	Double-well
γ_{MC}	1.0	1.013 ± 0.005	1.66 ± 0.02	1.74 ± 0.02	1.83 ± 0.07
γ	1.0	0.999 ± 0.005	1.64 ± 0.01	1.78 ± 0.01	1.96 ± 0.07
K_c	0.25	0.25	0.2989 ± 0.001	0.3288 ± 0.002	0.3722 ± 0.002
β_c	1.0	1.0	1.2142 ± 0.006	0.3288 ± 0.002	0.4305 ± 0.002
$c(2-\alpha)^2$	1.004 ± 0.005	0.999 ± 0.07	1.96 ± 0.04	1.94 ± 0.07	1.94 ± 0.09

[a] Error bars of γ and $c(2-\alpha)^2$ are only the fitting errors which represent the deviation from straight lines; other types of errors are involved; the error bar for K_c is estimated from the extrapolation of MC points near K_c. The first row of γ_{MC} estimates is calculated by using the absolute value definition of X_{MC} as in Eq. (30) and the second row is calculated by using Eq. (31) with $\langle X \rangle = 0$.

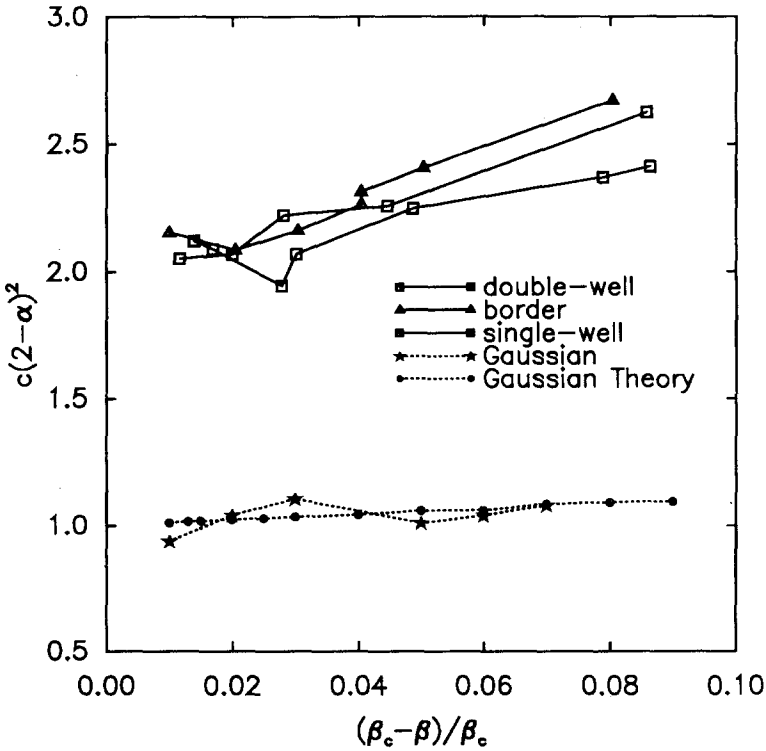

Fig. 12. $c(2-\alpha)^2$ for the different models studied. For the single-well model, the border model, and the double-well model, the result for $c(2-\alpha)^2$ is fairly close to 2 with fairly large error bars, as can be seen from the plot. However, they are well separated from the result of the Gaussian model, where the $\phi^4_{i,j}$ term is absent.

of $\langle |\varepsilon_{\mathbf{k}}|^2 \rangle$ for different models by the eighth-order polynomial fitting procedure. The region of $\mathbf{k}$ fitted is chosen to be the same as for the Gaussian model test. Though we expect that the K_c obtained from the 128×128 system is different from the true K_c for an infinite system, we here choose $K_{c,N}$ instead of K_c to calculate $c(2-\alpha)^2$ with the $K_{c,N}$ obtained from the 128×128 system, where $\langle |\varepsilon_{\mathbf{k}}|^2 \rangle$ reaches its peak value for the same $K_{c,N}$. The results of our calculations are plotted in Fig. 12.

6. DISCUSSION

In summary, we introduced a Monte Carlo scheme to study the universality behavior of 2D systems. We did not use the conventional finite-size scaling method. This scheme explicitly makes use of the results from the latest conformal theory which allows one to calculate the conformal charge of the system from the bulk property of the system near the critical point. We applied this method to the continuous-spin $\phi^4_{i,j}$ system, which is an important problem in itself. We studied the system in different parameter regions, ranging from the known Gaussian limit through the single-well model and the border model to the double-well model. We calculated the order parameter, energy, specific heat, and susceptibility. From our results we extracted estimates of the critical exponents, such as α and γ, and we calculated the conformal charge from the measurement of the energy–energy correlation functions.

In particular, we paid attention to the universality crossover from the Gaussian limit to the Ising limit. Although our study cannot be considered to be conclusive, it nonetheless provides us with a significant amount of information.

One important insight to the crossover behavior can be seen from our results on the specific heat study as shown in Fig. 10. Far from criticality, the energy fluctuations behave roughly the same (this fact is related to our choice of the normalization $\langle \phi^2_{i,j} \rangle = 1$ in our calculations). As we approach the critical point, the different curves start to deviate from each other; the specific heat of the Gaussian model diverges much faster than does that for the single-well model, the border model, and the double-well model.

One can explain this result as follows. As the critical point is approached, the large-amplitude fluctuations dominate the energy–energy fluctuations. The $\phi^4_{i,j}$ term would eventually control the energy–energy fluctuations and suppress this large-amplitude fluctuation irrespective of the details of the small-amplitude fluctuations. Without the suppression of the energy–energy fluctuations in the Gaussian limit from the $\phi^4_{i,j}$ term, there is a dramatic difference from the rest of the models.

The result of the conformal charge calculation for the Gaussian model is again well separated from the rests of the models, as can be seen from Fig. 12.

Within our error bars (systematic and statistical), there are still many possibilities for combinations of c and α, so that $c(2-\alpha)^2$ is consistent with the results of our calculations. From the results we have calculated, we cannot exclude, among other conformally invariant cases, the possibility that the Ising model universality class is valid for all $G>0$. Alternate cases include, for example, the case $c=0.7$, $\gamma=1.75$, $\alpha=0.25$, $c(2-\alpha)^2=2.14375$, which is allowed by conformal invariance. The independent determination of an additional critical index could help discriminate between variations in c and those in α. As we have seen, however, the accurate determination of α is difficult numerically, even in the Gaussian model. The usual problem that has been observed before by many workers is that, in these models, the divergence of the specific heat is relatively small and is hard to separate clearly from the analytic background. At least, however, a great number of possibilities can be excluded by our calculations.

ACKNOWLEDGMENTS

We would like to thank J. E. Gubernatis and D. K. Campbell for very important discussions. We thank the Advanced Computing Laboratory at Los Alamos National Laboratory for the use its facilities. This work could not have been completed without its generous support.

REFERENCES

1. A. A. Belavin, A. M. Polyakov, and A. B. Zamolodchikov, *Nucl. Phys. B* **241**:333 (1984).
2. J. L. Cardy, *Nucl. Phys. B* **240**[FS12]:514 (1984).
3. D. Friedan, Z. Qiu, and S. Shenker, *Phys. Rev. Lett.* **52**:1575 (1984).
4. J. L. Cardy, *J. Phys. A* **17**:L385 (1984).
5. H. W. J. Blöte, J. L. Cardy, and M. P. Nightingale, *Phys. Rev. Lett.* **56**:742 (1986).
6. I. Affleck, *Phys. Rev. Lett.* **56**:746 (1986).
7. A. B. Zamolodchikov, *JEPT Lett.* **43**:730 (1986).
8. J. L. Cardy, *Phys. Rev. Lett.* **60**:2709 (1988).
9. R. R. P. Singh and G. A. Baker, Jr., *Phys. Rev. Lett.* **66**:1 (1991); G. A. Baker, Jr., and R. R. P. Singh, *Physica A* **177**:123 (1991).
10. J. L. Cardy, in *Phase Transitions and Critical Phenomena*, Vol. 11, C. Domb and J. L. Lebowitz, eds. (Academic Press, London, 1987), p. 55.
11. G. A. Baker, Jr., *J. Math. Phys.* **24**:143 (1983); *J. Phys. A* **17**:L621 (1984); G. A. Baker, Jr., and J. D. Johnson, *J. Phys. A* **17**:L275 (1984).
12. M. Barma and M. E. Fisher, *Phys. Rev. Lett.* **53**:1935 (1984); *Phys. Rev. B* **31**:5954 (1985).
13. G. A. Baker, Jr., *Phys. Rev. Lett.* **60**:1844 (1988).
14. A. Milchev, D. W. Heermann, and K. Binder, *J. Stat. Phys.* **44**:749 (1986).
15. R. Toral and A. Chakrabari, *Phys. Rev. B* **42**:2445 (1990).

16. A. D. Bruce, *J. Phys. A* **18**:L873 (1985).
17. G. A. Baker, Jr., and J. M. Kincaid, *J. Stat. Phys.* **24**:469 (1981).
18. Xidi Wang, D. K. Campbell, and J. E. Gubernatis, Symmetry breaking in a quantum double-well chain: Application to hydrogen bonded materials, in preparation.
19. S. Duane, *Nucl. Phys. B* **257**:652 (1985); S. Duane and J. B. Kogut, *Nucl. Phys. B* **275**:398 (1986); S. Duane, A. D. Kennedy, B. J. Pendelton, and D. Roweth, *Phys. Lett. B* **195**:216 (1987).
20. A. E. Ferdinand, Thesis, Cornell University, Ithaca, New York (1967).
21. G. A. Baker, Jr., and J. D. Johnson, *J. Phys. A* **17**:L275 (1985).